Journal of Solid State Chemistry 184 (2011) 1339–1345

Contents lists available at ScienceDirect

Journal of Solid State Chemistry

journal homepage: www.elsevier.com/locate/jssc

Two new frameworks of potassium saccharate obtained from acidic and alkaline solution

Yao-Kang Lv, Yun-Long Feng*, Ji-Wei Liu, Zhan-Guo Jiang

Zhejiang Key Laboratory for Reactive Chemistry on Solid Surfaces, Institute of Physical Chemistry, Zhejiang Normal University, Jinhua, Zhejiang 321004, China

ARTICLE INFO

Article history:
Received 28 October 2010
Received in revised form
22 March 2011
Accepted 27 March 2011
Available online 5 April 2011

Keywords:
K(I) complexes
D-saccharic acid
Topology
Cyclic voltammetry
Nickel hydroxide electrode
Discharge curves

ABSTRACT

Two chiral K(I) complexes based on D-saccharic acid (H_2sac), $[K(Hsac)]_n$ (**1**) and $[K_2(sac)]_n$ (**2**) were obtained from acidic and alkaline solution. The 3D framework of **1** includes K(I) polyhedral rods and typical pairwise coaxial right- and left-handed helical chains, and displays binodal 6-connected pcu topology. **2** contains 2D polyhedral sheets consisting of left-handed helical chains, and generates 3D network with an unprecedented (7,11)-connected net. Cyclic voltammetry tests and charge–discharge tests indicate that the addition of complex **2** to the electrolyte could improve the electrochemical properties of the nickel hydroxide electrode.

1. Introduction

Helical assemblies are prevalent in biological systems and play key roles in molecular recognition, replication, and catalysis [1]. These facts have aroused the interests to design and synthesize coordination complexes containing helix. Several approaches have been developed for constructing helical complexes of potential applications [2], to date, the self-assembly of helical structure is still a challenging subject to chemists for the difficulty of selection of optimal components. Inspired by the aforementioned considerations, we aimed to couple our interest in obtaining new helical complexes via linking metal centers with chiral flexible ligands [3]. D-saccharic acid (H_2sac) (Scheme 1), which can be obtained from the oxidation of D-glucose, is a chiral flexible multidentate ligand and attractive as an excellent building blocks for the construction of metal coordination networks [4]. Due to the variable coordinate modes of this ligand, chemically similar complexes with diverse structure could be obtained from different experimental condition. In 1977, Taga et al. [5] reported a crystal structure of monopotassium saccharate K(Hsac), and in 2002, Styron et al. [6] reported another crystal structure of dipotassium saccharate monohydrate $K_2(sac)\cdot H_2O$. In this work, we reported two new K(I) complexes based on D-saccharic acid, $[K(Hsac)]_n$ (**1**) and $[K_2(sac)]_n$ (**2**) with novel helical chains.

In recent years, considerable attention has been paid to Ni/MH batteries for their high discharge capacity, high charge/recharge rate, environmental friendliness, reasonable price, etc. [7]. Up to now, most of the studies of Ni/MH batteries focus on electrode materials composition, molecular structure, morphology, kinetic property and so on [8]. But the effect of electrolyte additive on the electrochemical properties of electrode is also important, and now few concerns. Zhu et al. [9] demonstrated the effects of the redox additive such as $K_4Fe(CN)_6$ on the charge–discharge performances and internal pressure of the Ni/MH batteries. Shen et al. [10] reported the influence about the addition of $Cu(OH)_2$ to the KOH alkaline electrolyte on the electrochemical properties of $La_{0.75}Mg_{0.25}Ni_{3.5}$ hydrogen storage alloy electrode. Herein the influence about the addition of complex **2** to the KOH alkaline electrolyte on the electrochemical properties of nickel hydroxide electrode was further investigated.

2. Experiment section

2.1. Materials and measurements

Spherical β-$Ni(OH)_2$ particles coated with 5 wt% $Co(OH)_2$ were purchased from Changsha Xinye Industrial Co., Ltd. (China). All other starting reagents were purchased commercially and used without further purification. Elemental analyses were performed on a Perkin-Elmer 2400II elemental analyzer. IR spectra were measured in KBr pellets on a Nicolet 5DX FT-IR spectrometer.

* Corresponding author. Fax: +86 579 82282269.
E-mail address: sky37@zjnu.edu.cn (Y.-L. Feng).

0022-4596/$ - see front matter © 2011 Elsevier Inc. All rights reserved.
doi:10.1016/j.jssc.2011.03.042

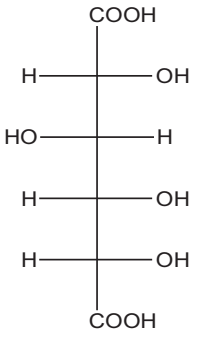

Scheme 1. D-saccharic acid (H_2sac).

2.2. Synthesis of [K(Hsac)]$_n$ (**1**)

D-saccharic acid potassium salt ([K(Hsac)]) purchased commercially were recrystallized from 25% of acetic acid, and colorless prism crystals suitable for X-ray diffraction studies were obtained. Elemental analysis calcd (%) for $C_6H_9KO_8$: C, 29.08; H, 3.70. Found: C, 29.03; H, 3.65. IR (KBr cm^{-1}): 3380(vs), 3264(vs), 2947(m), 1745(s), 1451(m), 1407(m), 1331(w), 1260(m), 1220(m), 1110(s), 1050(m), 945(w), 856(m), 656(s), 494(w).

2.3. Synthesis of [K_2(sac)]$_n$ (**2**)

Dissolve 0.124 g of **1** in 20 mL 7 mol L^{-1} KOH solution. The colorless microcrystalline powder was separated from the filtrate in three weeks. Crystals suitable for X-ray diffraction studies were recrystallized from N,N-dimethylformamide (DMF). The yield was about 57%. Elemental analysis calcd (%) for $C_6H_8K_2O_8$ (%): C, 25.20; H, 2.88. Found: C, 25.17; H2.82. IR (KBr cm^{-1}): 3420(vs), 3030(m), 2920(m), 2850(m), 1960(w), 1870(w), 1740(w), 1670(m), 1610(s), 1560(m), 1500(m), 1420(s), 1380(m), 1220(s), 1070(m), 1010(s), 802(m), 609(s), 513(m).

2.4. Single-crystal structure determination

The data collection of complexes **1** and **2** was performed on a Bruker APEX II diffractometer equipped with a graphite-monochromatized Mo-$K\alpha$ radiation (λ=0.71073 Å) at 296(2) K. Data intensity was corrected by Lorentz-polarization factors and empirical absorption. The structures were solved by direct methods and expanded with difference Fourier techniques. All non-hydrogen atoms were refined anisotropically. Except the hydrogen atoms on oxygen atoms were located from the difference Fourier maps, the other hydrogen atoms were generated geometrically. All calculations were performed using SHELXS-97 and SHELXL-97 [11]. Further details for structural analyses are summarized in Table 1, selected bond lengths and angles are listed in Table S1 and Table S2, the hydrogen bond distances and bond angles are listed in Table S3 and S4, respectively. CCDC – 689246 and 703535 contains the crystallographic data in CIF format.

2.5. Electrochemical evaluation

Nickel hydroxide electrodes were prepared by inserting an active paste into a nickel foam substrate. A paste containing 85 wt% active materials (5 wt% Co(OH)$_2$-coated nickel hydroxide spherical powder), 10 wt% carbon black and 5 wt% poly(tetrafluoroethylene) (PTFE) was used. The electrode was dried at 80 °C for 1 h and cut into a disk (1.0 × 2.0 cm^2), which was pressed at a pressure of 100 kg cm^{-2} to a thickness of 0.4 mm. Then the electrode was spot-welded to a nickel sheet for electrical connection. Cyclic voltammetry tests were carried out in a classical three-electrode cell with an electrochemistry work station (CHI650C, Chenhua instrument Ltd., Shanghai). The working electrode was the as-prepared nickel hydroxide electrode, the counter electrode was a nickel foil, and the reference electrode was an Hg/HgO electrode. For comparing, four kinds of electrolyte were used, 7 mol L^{-1} KOH solution, 7 mol L^{-1} KOH solution with the addition of 0.01 mol L^{-1} complex **2**, 7 mol L^{-1} KOH solution with the addition of 0.02 mol L^{-1} complex **2** and 7 mol L^{-1} KOH solution with the addition of 0.05 mol L^{-1} complex **2**. Using a Neware battery program-controlled test system, the charge–discharge tests were performed at 20 °C in a half-cell consisting of a working electrode (as-prepared nickel hydroxide electrode) and a counter electrode (a metal hydride electrode with excess capacity). There were four kinds of electrolyte: 7 mol L^{-1} KOH solution, 7 mol L^{-1} KOH solution with the addition of 0.01 mol L^{-1} complex **2**, 7 mol L^{-1} KOH solution with the addition of 0.03 mol L^{-1} complex **2** and 7 mol L^{-1} KOH solution with the addition of 0.05 mol L^{-1} complex **2**. The nickel hydroxide electrodes were charged at a rate of 0.2 C for 7.5 h, standed for 1 h and discharged at a 0.2 C rate to 0.9 V. Morphology of nickel hydroxide electrodes were also detected by field emission scanning electron microscopy (FE-SEM, Hitachi S-4800).

Table 1
Crystal data and structure refinement for **1** and **2**.

Complexes	1	2
Empirical formula	$C_6H_9KO_8$	$C_6H_8K_2O_8$
Formula weight	248.23	286.32
Crystal system	Monoclinic	Orthorhombic
Space group	$P2_1$	$P2_12_12_1$
a (Å)	4.8417 (2)	7.06520 (10)
b (Å)	10.8136 (6)	8.26060 (10)
c (Å)	8.4630 (5)	16.2660 (3)
β (deg.)	91.413 (4)	
V (Å^3)	442.96 (4)	949.33 (2)
Z	2	4
D/g (cm^{-3})	1.861	2.003
μ (mm^{-1})	0.63	1.03
GOF on F^2	1.000	1.000
$R1$, w$R2$ [$I > 2\sigma(I)$]	0.0238, 0.0642	0.0183, 0.0474
$R1$, w$R2$ (all data)	0.0248, 0.0657	0.0190, 0.0481

$R1 = [\Sigma|F_o| - |F_c|]/[\Sigma|F_c|]$. $wR2 = \{[\Sigma w(F_o^2 - F_c^2)^2]/[\Sigma w(F_o^2)^2]\}^{1/2}$.

3. Results and discussion

3.1. Crystal structure

Single-crystal X-ray diffraction analysis shows that complex **1** is monoclinic with chiral space group $P2_1$ with absolute structure Flack factors of 0.01(4). The asymmetric unit consists of one K(I) center and one Hsac$^-$ ligand. The K(I) cation is coordinated by nine oxygen atoms from six Hsac$^-$ ligands, forming a distorted monocapped square antiprism geometry (Fig. 1). All of the bond lengths of K–O vary considerably from 2.747(6) to 3.327(7) Å (Table S1), which are in agreement with those in the previously reported complexes [12]. The neighboring K(I) polyhedral share an edge to form an infinite rod-shaped chain, in which the adjacent K⋯K distance is 4.842(3) Å. Each Hsac$^-$ ligand adopts the unusual μ_6, η^2:η^2:η^1:η^1:η^1:η^1 coordination mode and binds to six K(I) cations through seven oxygen atoms from two bidentate carboxyl groups, one α-hydroxyl group and two β-hydroxyl group to generate two-dimensional (2D) wavy sheets around bc plane. The sheets are further interconnected by the K(I) polyhedral rods which stacked in parallel along a-axis, and complete the construction of the three-dimensional (3D) framework (Fig. 2). It is worth noting that K(I) is bridged by two bidentate carboxyl groups [O1–C1–O2] and

[O7–C6–O8] to generate pairwise coaxial right- and left-handed metal-carboxylate $[K(-OCO-)]_\infty$ helical chains, respectively. There are some reported examples of metal-organic coordination complexes with left- and right-handed helical chains, most of these helical chains are separated and alternately linked via hydrogen bonds, $\pi-\pi$ stacking interactions or covalence bonds [13]. In complex **1**, the pairwise coaxial helical chains cross at K(I) and their winding axis corresponds to the *b*-axis with the pitch length of 21.6272 Å. What's more, there are persistent O–H···O and C–H···O hydrogen bond (Table S3) to stabilize the crystal structure.

From a topological view, each $Hsac^-$ ligand is linked to six K(I) centers to result in a six-connected node (Fig. 3a), and each K(I) center is viewed as a six-connected node by combining six $Hsac^-$ ligands (Fig. 3b). Thus a (6,6)-connected pcu-type network is formed with Schläfli symbol of $4^{12}6^3$.

X-ray analysis revealed that complex **2** crystallizes in the orthorhombic chiral space group $P2_12_12_1$ with absolute structure Flack factor of 0.01(3). As shown in Fig. 4, the asymmetric unit consists of two K(I) centers and one sac^{2-} ligand. The sac^{2-} ligand has the μ_{10}, $\eta^2:\eta^2:\eta^1:\eta^2:\eta^3:\eta^1:\eta^3:\eta^2$ coordination mode which binds to five K1 atoms and five K2 atoms through eight oxygen atoms from two bidentate carboxyl groups, two α-hydroxyl group, and two β-hydroxyl group. Each K(I) atom is eight-coordinated with eight oxygen atoms from five sac^{2-}

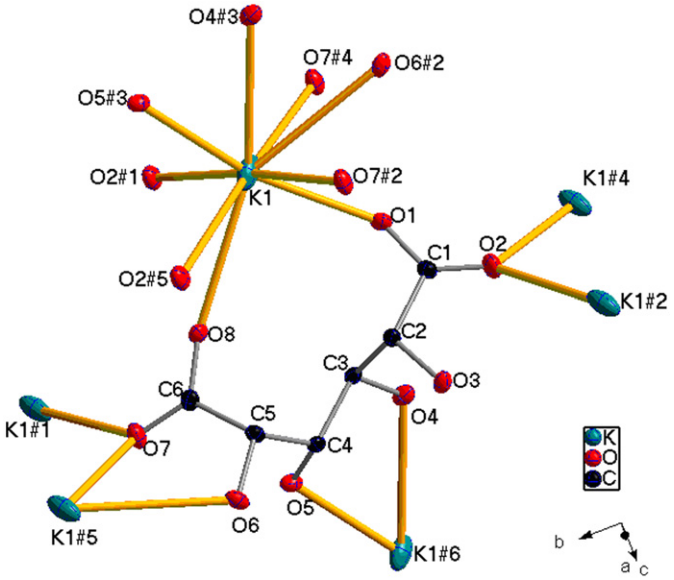

Fig. 1. Structure unit of **1** showing the atom labeling. Thermal ellipsoids are shown at the 30% probability level. All H atoms are omitted for clarity. Symmetry codes: (#1) $-x, y+1/2, -z$; (#2) $-x+1, y-1/2, -z$; (#3) $x, y, z-1$; (#4) $-x, y-1/2, -z$; (#5) $-x+1, y+1/2, -z$; (#6) $x, y, z+1$.

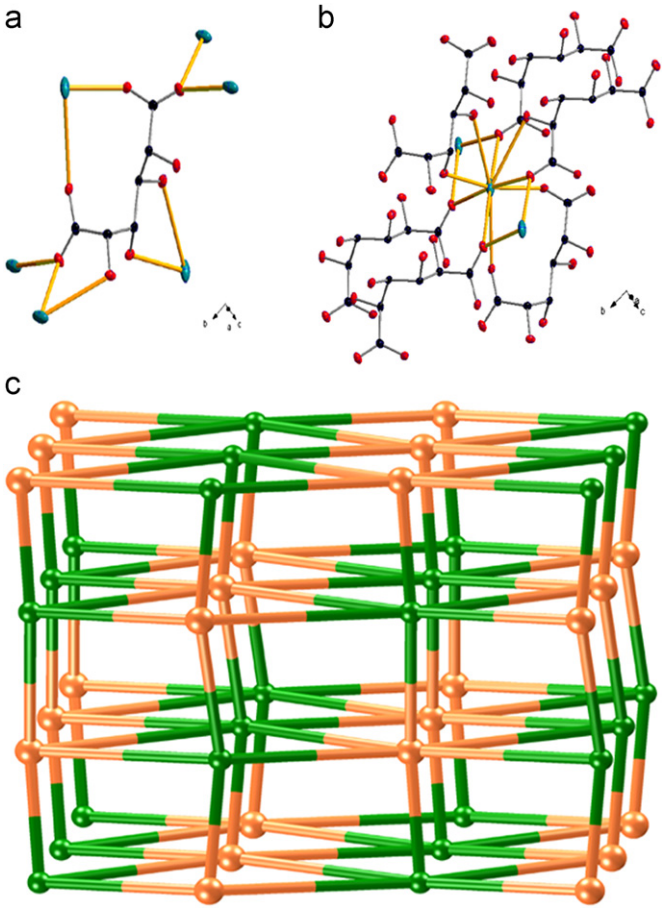

Fig. 3. (a) 6-connected $Hsac^-$ ligand linked with six K(I) units. (b) 6-connected K(I) units coordinated with six $Hsac^-$ ligands. (c) Schematic representation of the pcu topology of **1**. Green spheres represent K(I) centers; yellow spheres represent the ligands. (For interpretation of the references to color in this figure legend, the reader is referred to the web version of this article.)

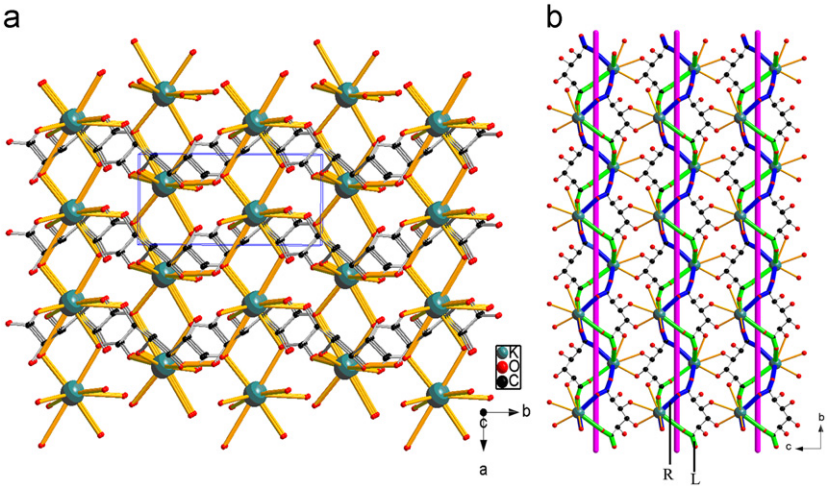

Fig. 2. (a) View of the framework for **1** down *c*-axis showing cell edges. (b) The 2D sheet of **1** constructed by 1D left- and right-handed pairwise coaxial helical chains following the 2_1 screw axis along *b*-axis.

ligands. K1 is coordinated by five carboxyl oxygen atoms from four different sac^{2-} ligands (K–O 2.658(4)–3.177(4) Å), three β-hydroxyl oxygen atoms from two different sac^{2-} ligands (K–O 2.712(6)–3.177(4) Å) in distorted dodecahedral geometry. K2 atom is coordinated by four carboxyl oxygen atoms, two α-hydroxyl oxygen atoms and two β-hydroxyl oxygen atoms in a distorted dodecahedron geometry. As illustrated in Fig. 5, each K1 dodecahedron shares a triangle plane with the closest K2 dodecahedron and form a secondary building unit (SBU) with K1···K2 distance of 3.7169(5) Å; each SBU connects to two neighboring SBUs through sharing a triangle plane and form an unusual left-handed inorganic 2_1 helical chain along the *b*-axis with a pitch of 8.2606(1) Å (Fig. 5a); helical chains share common edges and form infinite 2D inorganic sheets around *ab* plane (Fig. 5b). These polyhedron sheets are furthermore interlinked by sac^{2-} ligands and generate a compact 3D framework (Fig. 6).

Better insight of this complicated 3D architecture can be achieved by topology analysis. As shown in Fig. 7, each SBU is linked to 7 sac^{2-} ligands and 4 neighboring SBUs to represent a 11-connected node (Fig. 7a), while each sac^{2-} ligand serves for a 7-connected node by combining seven SBUs (Fig. 7b). Thus, a non-interpenetrating (7,11)-connected network is formed with Schläfli symbol of ($3^7.4^{10}.5^4$) ($3^{14}.4^{22}.5^{14}.6^5$). (Fig. 7d), the extended point symbol calculation using TOPOS 4.0 [14a] gives (3. 3. 3. 3. 3. 3. 3. 4. 4. 4. 4. 4_2. 4_2. 4_3. 4_3. 4_3. 4_3. 5_3. 5_3. 5_7. 5_7) for the 7-connected node, and (3. 3. 3. 3. 3. 3. 3. 3. 3. 3. 3. 3. 3. 3. 3. 4. 4. 4. 4. 4. 4. 4. 4. 4. 4. 4. 4. 4_2. 4_2. 4_2. 4_2. 4_3. 4_3. 4_3. 4_3. 4_3. 4_3. 4_3. 5_2. 5_2. 5_4. 5_4. 5_4. 5_4. 5_5. 5_5. 5_6. 5_6. 5_6. 5_6. 5_6. 6_{11}. 6_{11}. 6_{13}. 6_{13}. 6_{20}) for the 11-connected node. As far as we know, this topology is completely new within coordination polymer chemistry. To date, topology types with high node degree are very rare [14]. Note that the RCSR database contains only 17 binodal nets that are not edge transitive and have a node degree larger than eight [14b] (they are: (9,20)-

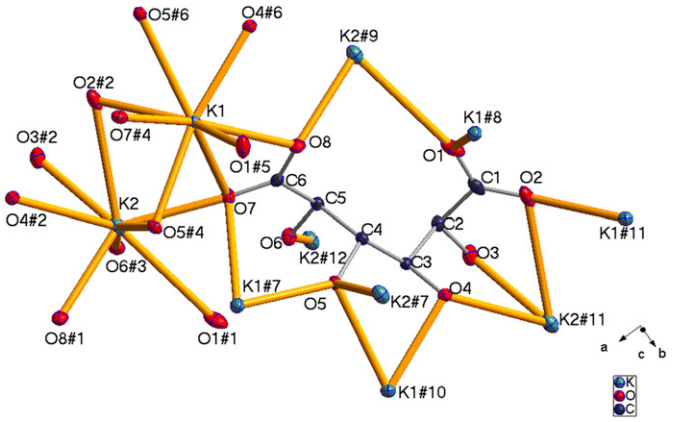

Fig. 4. Structure unit of **1** showing the atom labeling; thermal ellipsoids are shown at the 30% probability level. All H atoms and lattice water molecules are omitted for clarity. Symmetry codes: (#1) $x+1, y, z$; (#2) $x+1, y-1, z$; (#3) $x+1/2, -y+1/2, -z$; (#4) $-x+1, y-1/2, -z+1/2$; (#5) $-x, y-1/2, -z+1/2$; (#6) $x, y-1, z$; (#7) $-x+1, y+1/2, -z+1/2$; (#8) $-x, y+1/2, -z+1/2$; (#9) $x-1, y, z$; (#10) $x, y+1, z$; (#11) $x-1, y+1, z$; (#12) $x-1/2, -y+1/2, -z$.

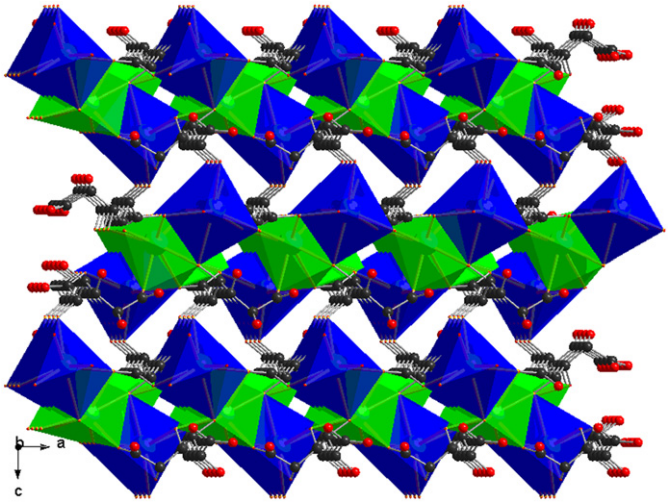

Fig. 6. View of the framework of **2** down *b*-axis, all H atoms have not been shown for clarity.

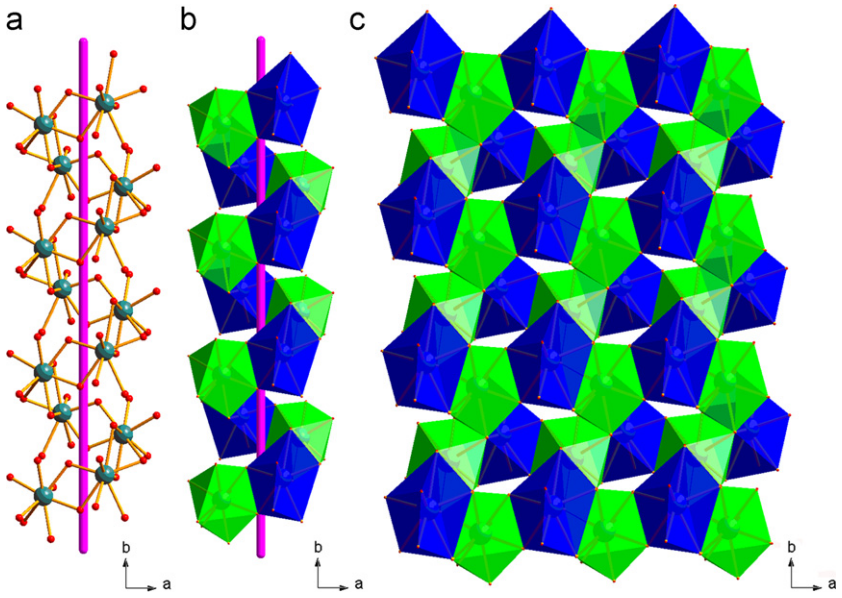

Fig. 5. (a) Ball-and-stick, (b) polyhedral representation of the left-handed polyhedral helical chain following the 2_1 screw axis along *b*-axis and (c) View of the polyhedral sheet down *c*-axis; green polyhedron represents the K1 dodecahedron, blue polyhedron represents the K2 dodecahedron. (For interpretation of the references to color in this figure legend, the reader is referred to the web version of this article.)

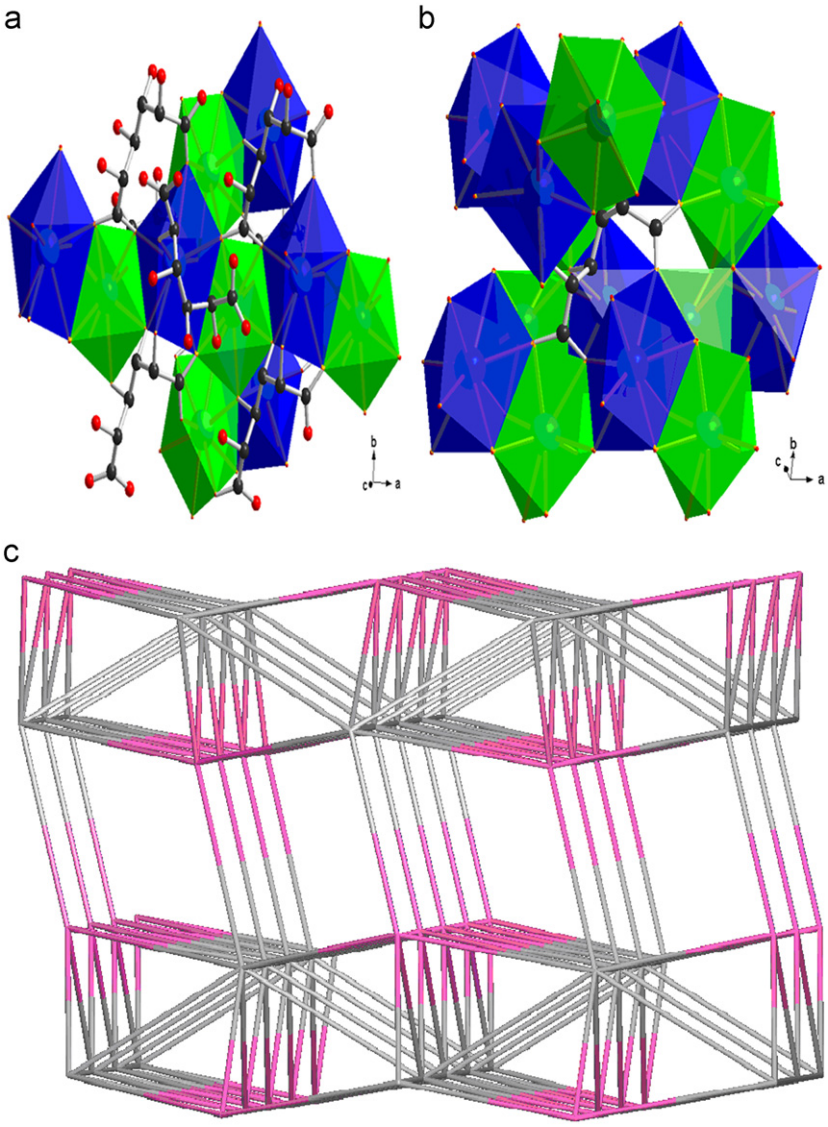

Fig. 7. (a) 10-connected SBU linked to 7 sac^{2-} ligands and 4 neighboring SBUs. (b) 7-connected sac^{2-} ligand coordinated with 7 SBUs. (c) Schematic representation of the binodal (7,11)-connected network of **2**.

alb-x, (6,18)-ast-d, (12,14)-bet, (12,15)-cla-d, (5,10)-fit, (3,9)-gfy, (10,12)-mbc, (12,16)-mgc-x, (8,14)-reo-d, (12,12)-tcj, (12,12)-tck, (12,12)-tcl, (12,12)-tcm, (10,10)-tcn, (10,10)-tco, (9,20)-tsl, (3,9)-xmz). The discovery of this new topology is useful at the basic level in the crystal engineering of coordination networks.

3.2. Electrochemical performance

Fig. 8 shows the cyclic voltammogram (CV) curves of the nickel hydroxide electrodes at scan rate of 0.1 V/s in (A) 7 mol L^{-1} KOH solution, (B) 7 mol L^{-1} KOH solution with the addition of 0.01 mol L^{-1} complex **2**, (C) 7 mol L^{-1} KOH solution with the addition of 0.03 mol L^{-1} complex **2** and (D) 7 mol L^{-1} KOH solution with the addition of 0.05 mol L^{-1} complex **2**, respectively. For comparison, the characteristic electrochemical parameters from CVs are summarized in Table 2. $\Delta E_{a,c}$, which is defined as the potential difference between the anodic and cathodic peaks, is used as a measure of the reversibility of the electrochemical redox reaction [15], the higher the reversibility, the smaller $\Delta E_{a,c}$ is. It can be seen that there is only one anodic (oxidation) and one cathodic (reduction) peak on the CV curves for both samples. The oxidation and reduction potential peaks of

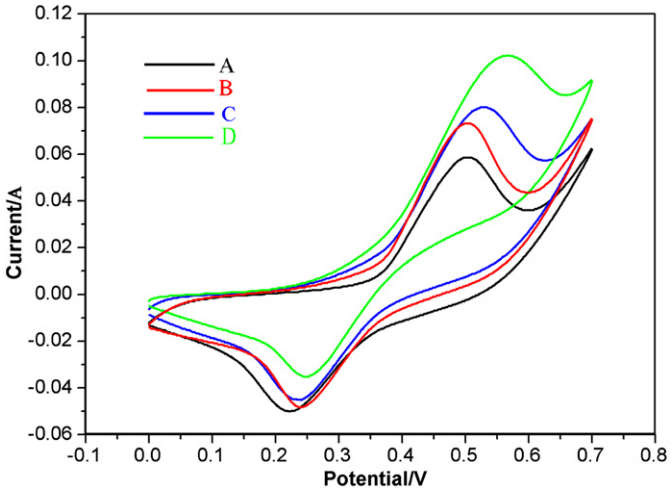

Fig. 8. CV of nickel hydroxide electrodes at scan rate of 0.1 V/s in (A) 7 mol L^{-1} KOH solution, (B) 7 mol L^{-1} KOH solution with the addition of 0.01 mol L^{-1} complex **2**, (C) 7 mol L^{-1} KOH solution with the addition of 0.03 mol L^{-1} complex **2** and (D) 7 mol L^{-1} KOH solution with the addition of 0.05 mol L^{-1} complex **2** at 20 °C.

nickel hydroxide electrode in 7 mol L^{-1} KOH solution (sample A) are at 0.503 and 0.222 V, respectively. The oxidation potential peak of nickel hydroxide electrode in 7 mol L^{-1} KOH solution containing 0.01 mol L^{-1} complex **2** (sample B) shifts to a more positive position at 0.504 mV and the reduction potential peak also moves to a more positive site at 0.239 mV. The potential difference, $\Delta E_{a,c}$, for the sample B is smaller than that of former one sample A, indicating good reversibility of the electrochemical redox reactions for sample B and the great facility of electron exchange in the electrode surface. Both of oxidation and reduction potential peaks shift to the positive direction as the concentration of complex **2** increased, but the potential difference of sample C (containing 0.03 mol L^{-1}) and sample D (containing 0.05 mol L^{-1}) are increased. At the same time, it is also found that the oxidation peak current increases significantly and linearly with the concentration of complex **2** in the range from 0.03 to 0.05 mol L^{-1}; while the reduction peak current of is reduced. Consequently, the electrochemical performance of Sample B is superior to the Sample A, Sample C and Sample D, suggesting that the adding appropriate complex **2** into 7 mol L^{-1} KOH solution could improve the electrochemical performance of nickel hydroxide electrode, but adding excessive complex **2** will depress the electrochemical performance.

Table 2
Electrochemical parameters from CVs of the sample peak potential.

Sample	Electrolyte	E_c (V)	E_a (V)	$\Delta E_{a,c}$ (V)
A	7 mol L^{-1} KOH	0.222	0.503	0.280
B	7 mol L^{-1} KOH+0.01 mol L^{-1} complex **2**	0.239	0.504	0.265
C	7 mol L^{-1} KOH+0.03 mol L^{-1} complex **2**	0.240	0.529	0.289
D	7 mol L^{-1} KOH+0.05 mol L^{-1} complex **2**	0.247	0.567	0.320

E_a and E_c are defined as the anodic (oxidation) peak potential and cathodic (reduction) peak potential, respectively.

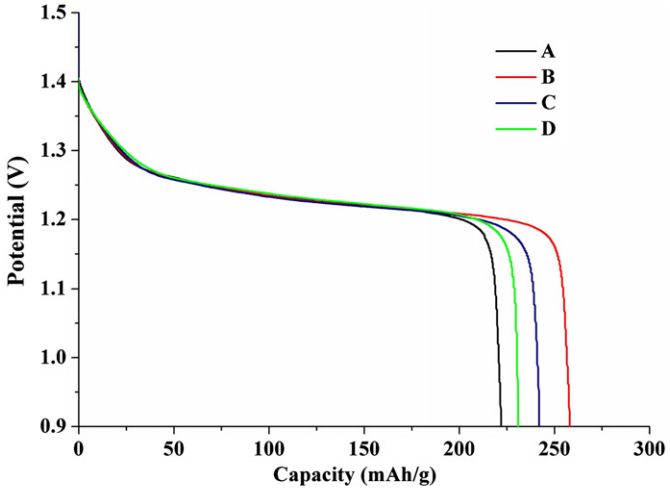

Fig. 9. Discharge curves as a function of capacity for nickel hydroxide electrodes in (A) 7 mol L^{-1} KOH solution, (B) 7 mol L^{-1} KOH solution with the addition of 0.01 mol L^{-1} complex **2**, (C) 7 mol L^{-1} KOH solution with the addition of 0.03 mol L^{-1} complex **2** at 20 °C and (D) 7 mol L^{-1} KOH solution with the addition of 0.05 mol L^{-1} complex **2** at 20 °C.

Discharge curves of nickel hydroxide electrodes in 7 mol L^{-1} KOH solution (sample A), 7 mol L^{-1} KOH solution containing 0.01 mol L^{-1} complex **2** (sample B), 7 mol L^{-1} KOH solution containing 0.03 mol L^{-1} complex **2** (sample C) and 7 mol L^{-1} KOH solution containing 0.05 mol L^{-1} complex **2** (sample D) at 20 °C are depicted in Fig. 9. The four samples have a similar single discharge potential plateau. Sample B exhibits the largest discharge capacity (258.0 mAh/g) in comparison with sample A (221.9 mAh/g), sample C (242.0 mAh/g) and sample D (230.8 mAh/g). at the same discharge rate. It can be found that, as an additive of electrolyte, the complex **2** can improve the discharge capacity of nickel hydroxide electrode. Complex **2** may be ionized into sac^{2-} ions in the electrolyte, which will adsorbed on the electrode surface during the charge–discharge cycles, and we speculate that these sac^{2-} ions would reduce the deformation of the electrode and the shedding of active material, thereby the electrochemical performance could be improved. However, adding excessive complex **2** will inhibit ion transport, reduce the exchange current density of electrolyte, and increase the resistance of the battery.

Fig. 10a shows the SEM micrograph of the surface of nickel hydroxide electrode after 5 charge–discharge cycles without addition of complex **2** in the electrolyte. It can be clearly seen that there are many cracks in the range of 2–15 μm and holes about 10 μm in diameter in the electrode surface, which have been created during the charge–discharge process. Fig. 10b shows the SEM micrograph of the surface of nickel hydroxide electrode with the addition of 0.01 mol L^{-1} complex **2** in the electrolyte after 5 charge–discharge cycles, it can be found that both the cracks and the holes are much fewer than Fig. 10b. These result indicated that as the addition of complex **2** would reduce the shedding of the positive active material and could give extended life cycle capacity consequently.

4. Conclusion

In summary, we have obtained two new structure of potassium saccharate from acidic and alkaline solution. The 3D framework of **1**

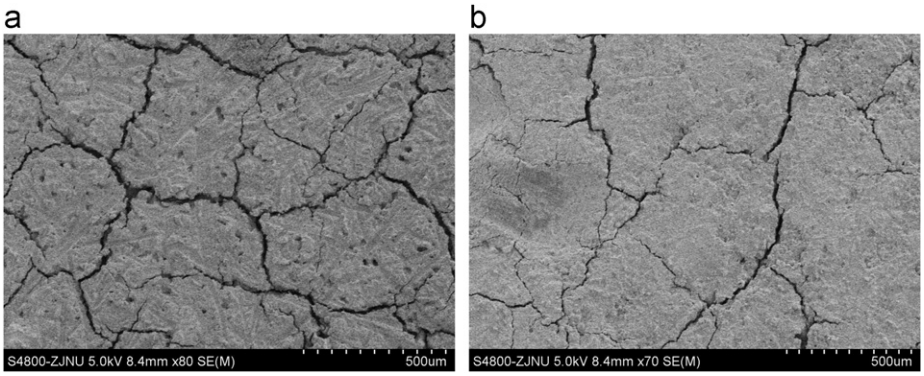

Fig. 10. SEM micrograph of the surface of nickel hydroxide electrode after 5 charge–discharge cycles (a) non-addition of complex **2** in the electrolyte (b) with the addition of 0.01 mol L^{-1} complex **2** in the electrolyte.

includes K(I) polyhedral rods and typical pairwise coaxial right- and left-handed helical chains and display binodal 6-connected pcu topology, while **2** contains 2D polyhedral sheets consist of right-handed polyhedral helical chains and generate 3D network with an unprecedented (7,11)-connected net. The CVs suggesting that adding appropriate complex **2** to 7 mol L^{-1} KOH solution could improve the electrochemical performance of nickel hydroxide electrode. And through discharge curves it is founded that the discharge capacity of the nickel hydroxide electrode is increased with the addition of 0.01 mol L^{-1} complex **2** to the electrolyte. The electrochemical and morphology studies indicated that the addition of complex **2** to the electrolyte could improve the electrochemical properties of the nickel hydroxide electrode.

Acknowledgments

The authors are grateful to the Science and Technology Department of Zhejiang Province for financial support of the project (2007C21174).

Appendix A. Supplementary material

Supplementary data associated with this article can be found in the online version at doi:10.1016/j.jssc.2011.03.042.

References

[1] (a) T.W. Bell, H. Jousselin, Nature 367 (1994) 441;
(b) S. Chatterjee, P.G. Vasudev, S. Raghothama, C. Ramakrishnan, N. Shamala, P. Balaram, J. Am. Chem. Soc. 131 (2009) 5956;
(c) D. Eisenberg, Proc. Natl. Acad. Sci. USA 100 (2003) 11207;
(d) S.C. Ha, K. Lowenhaupt, A. Rich, Y.G. Kim, K.K. Kim, Nature 437 (2005) 1183;
(e) Y. Hase, K. Nagai, H. Iida, K. Maeda, N. Ochi, K. Sawabe, K. Sakajiri, K. Okoshi, E. Yashima, J. Am. Chem. Soc. 131 (2009) 10719;
(f) O.S. Jung, Y.J. Kim, Y.A. Lee, J.K. Park, H.K. Chae, J. Am. Chem. Soc. 122 (2000) 9921;
(g) G.W. Orr, L.J. Barbour, J.L. Atwood, Science 285 (1999) 1049;
(h) Z.Q. Wu, K. Nagai, M. Banno, K. Okoshi, K. Onitsuka, E. Yashima, J. Am. Chem. Soc. 131 (2009) 6708.
[2] (a) S.P. Anthony, T.P. Radhakrishnan, Chem. Commun. (2004) 1058;
(b) B.L. Chen, S.Q. Ma, E.J. Hurtado, E.B. Lobkovsky, H.C. Zhou, Inorg. Chem. 46 (2007) 8490;
(c) B.L. Chen, S.Q. Ma, F. Zapata, F.R. Fronczek, E.B. Lobkovsky, H.C. Zhou, Inorg. Chem. 46 (2007) 1233;
(d) Y. Cui, S.J. Lee, W.B. Lin, J. Am. Chem. Soc. 125 (2003) 6014;
(e) A.D. Cutland-Van Noord, J.W. Kampf, V.L. Pecoraro, Angew. Chem. Int. Ed. 41 (2002) 4667;
(f) Q. Gao, M.Y. Wu, Y.G. Huang, L. Chen, W. Wei, Q.F. Zhang, F.L. Jiang, M.C. Hong, CrystEngComm. 11 (2009) 1831;
(g) X.J. Gu, D.F. Xue, Inorg. Chem. 45 (2006) 9257;
(h) T.H. Noh, Y.J. Choi, Y.K. Ryu, Y.A. Lee, O.S. Jung, CrystEngComm. 11 (2009) 2371.
[3] (a) Y.H. He, Y.L. Feng, Y.Z. Lan, Y.H. Wen, Cryst. Growth Des. 8 (2008) 3586;
(b) X.H. Geng, Y.L. Feng, Y.Z. Lan, Inorg. Chem. Commun. 12 (2009) 447;
(c) Y.H. He, Y.Z. Lan, C.H. Zhan, Y.L. Feng, H. Su, Inorg. Chim. Acta 362 (2009) 1952;
(d) J.L. Yin, Y.L. Feng, Y.Z. Lan, Inorg. Chim. Acta 362 (2009) 3769;
(e) Y.K. Lv, C.H. Zhan, Y.L. Feng, CrystEngComm. 12 (2010) 3052;
(f) Y.K. Lv, C.H. Zhan, Z.G. Jiang, Y.L. Feng, Inorg. Chem. Commun. 13 (2010) 440;
(g) Y.K. Lv, J. Chen, X.J. Wang, Y.L. Feng, Chin. J. Struct. Chem. 29 (2010) 1483.
[4] (a) B.F. Abrahams, M. Moylan, S.D. Orchard, R. Robson, Angew. Chem. Int. Ed. 42 (2003) 1848;
(b) F. Ferrier, A. Avezou, G. Terzian, D. Benlian, J. Mol. Struct. 442 (1998) 281;
(c) A. Lakatos, R. Bertani, T. Kiss, A. Venzo, M. Casarin, F. Benetollo, P. Ganis, D. Favretto, Chem. Eur. J. 10 (2004) 1281.
[5] T. Taga, Y. Kuroda, K. Osaki, Bull. Chem. Soc. Jpn. 50 (1977) 3079.
[6] S.D. Styron, A.D. French, J.D. Friedrich, C.H. Lake, D.E. Kiely, J. Carbohydr. Chem. 21 (2002) 27.
[7] (a) M. Armand, J.M. Tarascon, Nature 451 (2008) 652;
(b) F. Ferrier, A. Avezou, G. Terzian, D. Benlian, J. Mol. Struct. 442 (1998) 281;
(c) G.W. Orr, L.J. Barbour, J.L. Atwood, Science 285 (1999) 1049;
(d) S.R. Ovshinsky, M.A. Fetcenko, J. Ross, Science 260 (1993) 176.
[8] (a) M. Casas-Cabanas, J. Canales-Vazquez, J. Rodriguez-Carvajal, M.R. Palacin, J. Am. Chem. Soc. 129 (2007) 5840;
(b) L.H. Dong, Y. Chu, W.D. Sun, Chem. Eur. J. 14 (2008) 5064;
(c) M. Douin, L. Guerlou-Demourgues, L. Goubault, P. Bernard, C. Delmas, J. Electrochem. Soc. 156 (2009) A459;
(d) A. Hande, J. Power Sources 158 (2006) 1039;
(e) S. Ida, D. Shiga, M. Koinuma, Y. Matsumoto, J. Am. Chem. Soc. 130 (2008) 14038;
(f) Y.K. Lv, Y.L. Feng, Chin. J. Inorg. Chem. 25 (2009) 447;
(g) W. Zhou, M. Yao, L. Guo, Y.M. Li, J.H. Li, S.H. Yang, J. Am. Chem. Soc. 131 (2009) 2959;
(h) B.H. Liu, S.H. Yu, S.F. Chen, C.Y. Wu, J. Phys. Chem. B 110 (2006) 4039;
(i) W.Y. Li, S.Y. Zhang, J. Chen, J. Phys. Chem. B 109 (2005) 14025.
[9] X.M. Zhu, H.X. Yang, X.P. Ai, Electrochim. Acta 48 (2003) 4033.
[10] X.Q. Shen, Y.G. Chen, M.D. Tao, C.L. Wu, G. Deng, Electrochim. Acta 54 (2009) 2581.
[11] (a) G.M. Sheldrick, SHELXS-97, Program for X-ray Crystal Structure Solution, University of Göttingen, Göttingen, Germany, 1997;
(b) G.M. Sheldrick, SHELXL-97, Program for X-Ray Crystal Structure Refinement, University of Göttingen, Göttingen, Germany, 1997.
[12] (a) A. Askarinejad, M.R. Fadaei, A. Morsali, A.R. Mahjoub, J. Coord. Chem. 60 (2007) 753;
(b) D. Braga, L. Maini, M. Polito, M. Rossini, F. Grepioni, Chem. Eur. J. 6 (2000) 4227;
(c) H.Y. Chen, T.L. Zhang, J.G. Zhang, L. Yang, J.Y. Guo, Struct. Chem. 17 (2006) 445;
(d) Q.L. Guo, Y.X. Qu, S.L. Ma, W.X. Zhu, Chem. J. Chin. Univ. 27 (2006) 2034;
(e) G.X. Ma, T.L. Zhang, J.G. Zhang, B. Shao, Y.F. Li, J.C. Song, K.B. Yu, Chin. J. Chem. 22 (2004) 131;
(f) H. Miyasaka, N. Matsumoto, H. Okawa, N. Re, E. Gallo, C. Floriani, Angew. Chem. Int. Ed. Engl. 34 (1995) 1446;
(g) H. Miyasaka, N. Matsumoto, H. Okawa, N. Re, E. Gallo, C. Floriani, J. Am. Chem. Soc. 118 (1996) 981;
(h) P. Thuery, B. Masci, M. Takimoto, T. Yamato, Inorg. Chem. Commun. 10 (2007) 795.
[13] (a) X.M. Chen, G.F. Liu, Chem. Eur. J. 8 (2002) 4811;
(b) M. Du, C.P. Li, X.J. Zhao, Cryst. Growth Des. 6 (2006) 335;
(c) X.Y. Duan, X. Cheng, J.G. Lin, S.Q. Zang, Y.Z. Li, C.J. Zhu, Q.J. Meng, CrystEngComm. 10 (2008) 706;
(d) Y.W. Hu, G.H. Li, X.M. Liu, B. Hu, M.H. Bi, L. Gao, Z. Shi, S.H. Feng, CrystEngComm. 10 (2008) 888;
(e) Y.J. Qi, Y.H. Wang, C.W. Hu, M.H. Cao, L. Mao, E.B. Wang, Inorg. Chem. 42 (2003) 8519;
(f) L. Xu, C. Qin, X.L. Wang, Y.G. Wei, E. Wang, Inorg. Chem. 42 (2003) 7342.
[14] (a) V.A. Blatov, TOPOS, A Multipurpose Crystallochemical Analysis with the Program Package, Russia, 2004.;
(b) V.A. Blatov, D.M. Proserpio, Acta Cryst. A 63 (2009) 329;
(c) V.A. Blatov, L. Carlucci, G. Giani, D.M. Proserpio, CrystEngComm. 6 (2004) 377;
(d) S.R. Batten, D.R. Turner, M.S. Neville, Coordination Polymers: Design, Analysis and Application, RSC, Cambridge, 2009;
(e) L. Öhrström, K. Larsson, Molecule-Based Materials. The Structural Network Approach, Elsevier, Amsterdam, 2005;
(f) M. O'Keeffe, M.A. Peskov, S.J. Ramsden, O.M. Yaghi, Acc. Chem. Res. 41 (2008) 1782;
(g) V.A. Blatov, Acta Cryst. A 63 (2007) 329;
(h) I.A. Baburin, V.A. Blatov, L. Carlucci, G. Cianib, D.M. Proserpio, CrystEngComm. 10 (2008) 1822;
(i) V.A. Blatov, M.V. Peskov, Acta Cryst. B 62 (2006) 457;
(j) A.F. Wells, Three-Dimensional Nets and Polyhedra, Wiley, New York, 1977;
(k) A.F. Wells, Further Studies of Three-dimensional Nets, ACA Monograph 8, American Crystallographic Association, Buffalo, NY, 1979;
(l) M. O'Keeffe, S.T. Hyde, Zeolites 19 (1997) 370;
(m) M. O'Keeffe, Nature 400 (1999) 617;
(n) N.W. Ockwig, O.D. Friedrichs, M. O'Keeffe, O.M. Yaghi, Acc. Chem. Res. 38 (2005) 176.
[15] (a) Q.D. Wu, X.P. Gao, G.R. Li, G.L. Pan, T.Y. Yan, H.Y. Zhu, J. Phys. Chem. C 111 (2007) 17082;
(b) D.A. Corrigan, R.M. Bendert, J. Electrochem. Soc. 136 (1989) 723.